Preparation and Properties of PDMS elastomer cross-linked with hydrolyzate of TEOS, HEDS, or OETS oligomers: influence of cross-linker structure

Yohei Sato
Tokyo University of Science
Ryohei Hayami
Tokyo University of Science
Kazuki Yamamoto
Tokyo University of Science
Takahiro Gunji (gunji@rs.tus.ac.jp)
Tokyo University of Science

Research Article

Keywords: Polysiloxane, Alkoxysilane, Oligosiloxane, Elastomer

Posted Date: August 21st, 2023

DOI: https://doi.org/10.21203/rs.3.rs-3266823/v1

Additional Declarations: No competing interests reported.

Version of Record: A version of this preprint was published at Journal of Sol-Gel Science and Technology on October 28th, 2023. See the published version at https://doi.org/10.1007/s10971-023-06247-y.

Abstract

Linear oligoethoxysiloxanes were hydrolyzed, and the resulting hydrolyzates were dimethylsilylated to produce Si–H terminated ethoxysiloxanes (CLs). These CLs were characterized using gel permeation chromatography, nuclear magnetic resonance, and Fourier-transform infrared spectroscopy. The results indicated the formation of highly condensed cyclic siloxanes, four-membered cyclic siloxanes, and linearly condensed cyclic siloxanes when derived from tetraethoxysilane, hexaethoxydisiloxane, and octaethoxytrisiloxane, respectively. The CLs were subsequently reacted with vinyl-terminated polydimethylsiloxane in the presence of the Karstedt catalyst to yield PDMS elastomers, which are comprised of di- and quadra-functional silicones. Tests for transmittance, thermal properties, tensile strength, and swelling in toluene were conducted to assess the impact of the molecular weight and microstructure of the CLs on the final products. As the number of silicon atoms in the linear oligoethoxysiloxanes increased, there was a noticeable rise in the secant modulus and a reduction in the degree of swelling. These findings suggest that the structure of PDMS elastomers can be tailored by varying the structure of the linear oligosiloxanes used as a cross-linking agent.

Highlights

- Si–H terminated ethoxysiloxanes were synthesized from hydrolyzates of tetraethoxysilane, hexaethoxydisiloxane, or octaethoxytrisiloxane and chloro(dimethyl)silane.
- PDMS elastomers were synthesized via the hydrosilylation of the Si–H terminated ethoxysiloxanes with vinyl-terminated polydimethylsiloxane.
- Secant modulus increased, while the degree of swelling decreased, with an increase in the number of silicon atoms in linear oligosiloxanes.
- Mechanical testing and the swelling test in toluene demonstrated that the structure of PDMS elastomers can be influenced by the structure of linear oligosiloxanes used as a cross-linking agent.Top of Form

1 Introduction

Organic–inorganic hybrid materials are composed of organic and inorganic components, offering the potential for novel functions and applications by combining the advantages of each component [1, 2]. Sanchez et al. proposed a classification for organic–inorganic hybrid materials based on the hybridization of organic and inorganic components, ranging from a few Ångstroms to several nanometers in length [3, 4]. Class I hybrid materials are characterized by weak interactions, such as van der Waals forces, hydrogen bonding, coordination bonding, electrostatic forces, among others, between the organic and inorganic segments. Conversely, Class II hybrid materials are formed through stronger interactions, like covalent and ionic bonds.

Our research has also delved into organic–inorganic hybrid materials. Examples include triethoxysilyl modified C_{60}, polyhedral oligomeric silsesquioxane, and titanium phosphonate clusters as inorganic segments, combined with hydroxy-terminated polydimethylsiloxane (PDMS) as the organic segment, resulting in Class II hybrid materials [5–7]. Notably, the siloxane/epoxy hybrid within Class II displayed enhanced physical properties, exhibiting high mechanical strength when the organic and inorganic polymers were joined through covalent bonds [8].

Recently, we discussed the hydrolysis-condensation reaction of linear ethoxyoligosiloxanes, known to form during the early stages of the sol–gel reaction of tetraethoxysilane (TEOS) [9]. Our findings indicate that TEOS, hexaethoxydisiloxane (HEDS), and octaethoxytrisiloxane (OETS) produce polymers with distinct characteristics: network-type polymers containing cyclic siloxanes, polymers containing cyclic siloxanes with four silicon atoms, and polymers containing various cyclic siloxanes, respectively. These results shed light on the structural and chemical variations in the starting materials. This type of findings suggest the potential application of linear ethoxyoligosiloxanes, both novel and conventional inorganic polymers with varying structures, as integral inorganic components in organic–inorganic hybrid materials. Moreover, to fine-tune the properties of PDMS-based hybrid materials, the structure of the inorganic segment is considered pivotal [10].

In this study, we explore the preparation and properties of PDMS silicone elastomers—recognized hybrids of di- and quadra-functional siloxanes. We realized this by cross-linking the vinyl-terminated PDMS with hydrolyzates of linear–ethoxyoligosiloxanes, demonstrating their cross-linking capability, as illustrated in Scheme 1.

2 Experimental sections

2.1 Measurements

Nuclear magnetic resonance (NMR) spectra were recorded using a JNM–ECZ 400 spectrometer (JEOL, Japan; ^{1}H: 399.00 MHz, ^{29}Si{^{1}H}: 79.00 MHz). The chemical shifts were reported in ppm relative to residual chloroform in deuterated chloroform ($CDCl_3$) (for ^{1}H: 7.26 ppm) and tetramethylsilane (for ^{29}Si{^{1}H}: 0.00 ppm) as the internal standards. For ^{29}Si{^{1}H} NMR spectra, chromium(III) acetylacetonate was added to the sample as a paramagnetic relaxation agent. Fourier–transform infrared (FTIR) spectra were recorded on a FT/IR–6100 spectrophotometer (JASCO, Japan) via the neat method, in which the sample is sandwiched between two KBr crystal disks, or via attenuated total reflectance (ATR) method using a JASCO ATR PRO 0450–S (ZnSe prism). Thermal gravimetric analysis (TGA) was performed using a TG-DTA analyzer 2000SE (Netzsch Japan, Japan) at a heating rate of 10°C min^{-1} up to 1000°C under nitrogen or air flow. Ultraviolet-visible (UV–Vis) transmittance spectra were recorded using a V-670 UV–VIS/NIR spectrophotometer (JASCO, Japan) with an integrating sphere (ISN–470 type). High-resolution electrospray ionization time–of–flight mass spectrometry (HR–ESI–TOF MS) was performed using a JMS-T100CS AccuTOF CS (JEOL, Japan). Gel permeation chromatography (GPC) was performed

using a LC-20AD HPLC prominence liquid chromatograph (Shimadzu, Japan) attached to a Plgel 5-μm Mixed–D column. Tetrahydrofuran (THF) was used as an eluent (1 mL min^{-1}), and a RID-20A was used as the detector at 40°C. The number–average molecular weight (M_n), weight–average molecular weight (M_w), and polydispersity (M_w/M_n) were calculated based on the standard polystyrene. The tensile strength test of samples, which were cut to a size of 30 mm × 5 mm, was evaluated using a MCT-2150 (A&D, Japan) at a tensile speed of 10 mm/min at approximately 23°C. A swelling test was evaluated by solvent uptake of samples immersed in toluene for 3 days. The degrees of swelling (DS) for the samples were calculated using the following equation: $DS\ (\%) = 100 \times (W_a - W_b)/W_b$

where W_a and W_b denote the weight after and before sample immersion, respectively.

2.2 Materials

Ethanol (EtOH), THF, toluene, and diethylether were purified via standard processes and stored over activated molecular sieves. Tetraisocyanatosilane was provided by Matsumoto Fine Chemical Co., Ltd (Japan). Octamethylcyclotetrasiloxane (D_4) was purchased from Shin–Etsu Chemical (Japan). Ammonium carbonate ($(NH_4)_2CO_3$) and potassium hydroxide (KOH) were purchased from Kanto Chemical Co., Inc. (Japan). *N*,*N*–Dimethylformamide (DMF) and 6 M hydrochloric acid (HCl aq.) were purchased from FUJIFILM Wako Pure Chemical Corporation (Japan). TEOS, thionyl chloride ($SOCl_2$), chlorodimethylsilane, and chlorodimethylvinylsilane were purchased from Tokyo Chemical Industry Co. Ltd (Japan). Karstedt catalyst (0.1 M in xylene solution) was purchased from Sigma-Aldrich (Tokyo, Japan). TEOS and tetraisocyanatosilane were purified by distillation. Hexaethoxydisiloxane (HEDS) and octaethoxytrisiloxane (OETS) were synthesized according to previous report [10]. KOH powder was prepared as follows: KOH pellets were dissolved in EtOH and reprecipitated with THF followed via drying under vacuum at 90°C for 3 h [11]. Dimethylvinylsiloxy terminated polydimethylsiloxane (PDMS–Vi) was prepared by the ring–opening polymerization of D_4 with KOH powder followed by silylation using chlorodimethylvinylsilane, and M_w and M_w/M_n of PDMS–Vi were 49,000 Da and 3.3, respectively. The preparation methods and characterization are provided in Supporting Information.

2.3 Synthesis of Si–H terminated oligosiloxane cross–linkers (CL_{TEOS}, CL_{HEDS}, CL_{OETS})

HCl aq. was slowly added to EtOH solution of ethoxysilane monomer (TEOS, HEDS, OETS). These molar ratios were HCl/Si = 0.1 (HCl/TEOS = 0.1, HCl/HEDS = 0.2, HCl/OETS = 0.3), H_2O/Si–OEt = 0.5 (H_2O/TEOS = 2, H_2O/HEDS = 3, H_2O/OETS = 4), and EtOH/Si = 10 (EtOH/TEOS = 10, EtOH/HEDS = 20, EtOH/OETS = 30). The mixture was stirred in an ice bath for 10 minutes. Then, the mixture was stirred for 3 h at room temperature (approximately 23°C). Chlorodimethylsilane (equimolar ratio of added H_2O) was added with stirring in an ice bath for 10 min. The mixture was poured into a mixed solvent of THF/hexane (1/2 v/v) followed by washing with water for twice and brine for twice. The organic layer was dried over anhydrous sodium sulfate, filtered, and then evaporated. The resulting Si–H terminated oligosiloxane cross-linkers were obtained as a colorless liquid.

CL_{TEOS}: M_w = 1,500 Da, M_w/M_n=1.1

CL_{HEDS}: M_w = 1,400 Da, M_w/M_n=1.1

CL_{OETS}: M_w = 1,200 Da, M_w/M_n=1.1

2.4 Preparation of PDMS-CLs

A 1-g mixture, containing PDMS–Vi and Si–H terminated oligosiloxane cross-linkers (at concentrations of 10wt%, 20wt%, and 40wt% relative to PDMS–Vi), was dissolved in 4 g of THF. To this solution, 10 µl of Karstedt catalyst (0.1 M in a xylene solution) was added and the mixture was stirred for 30 min. Subsequently, the mixture was poured into a 50-mm ϕ Teflon Petri dish. It was then cured at 50°C for one day, followed by heating at 150°C for an additional day.

3 Results and discussion

3.1 Characterization of Si–H terminated oligosiloxane cross–linkers (CLs)

The $^{29}Si\{^1H\}$ NMR spectra of the hydrolysis condensates of TEOS, HEDS, and OETS, before and after silylation, are presented in Fig. 1. Prior to silylation, all hydrolysis condensates primarily displayed signals corresponding to the 4-membered cyclic $Q^2(OEt)(OH)$ (-92.7 ppm) and 4-membered cyclic $Q^2(OEt)_2$ (-95.1 ppm). Minor signals associated with $Q^1(OEt)_2(OH)$ (around − 86 ppm), cyclic $Q^2(OH)_2$ (-90.6 ppm), Q^3–OH (-99.6 to -101 ppm), and Q^3–OEt (-101.5 to -103 ppm) were also observed [10, 12–14]. Small signals due to 5- or 6-membered cyclic $Q^2(OEt)_2$ (-95.4 ppm) were evident in the hydrolysis condensates of TEOS and OETS before silylation [11, 15]. Following silylation, complex signals attributed to the dimethylsiloxyl group emerged between − 1 to -5 ppm [12]. All the silylated hydrolyzates—CL_{TEOS}, CL_{HEDS}, and CL_{OETS} included end-group $Q^1(OEt)_3$ (-89.0 ppm), 4-membered cyclic $Q^2(OEt)_2$ (-95.3 ppm), and linear $Q^2(OEt)_2$ (-96.5 ppm). The Q^3 and Q^4 units were evident between − 99 to -105 ppm and − 105 to -110 ppm, respectively, but their detailed structures remained unidentified. Table 1 provides GPC results, OEt/Si-H ratios, siloxane unit ratios, and the degree of crosslinking (DC). The OEt/Si-H ratios of the CLs showed no discernible differences.

Table 1. Synthesis of CLs

monomer	Before/after silylation	GPC result[a]		OEt/Si-H[b]	Ratio of siloxane units[c](%)					DC[d] (%)
		$M_w \times 10^{-3}$	M_w/M_n	ratio	Q^0	Q^1	Q^2	Q^3	Q^4	
CL_{TEOS}	Before				0	11	44	45	0	59
	After	1.5	1.1	4	0	4	36	44	16	68
CL_{HEDS}	Before				0	8	48	44	0	59
	After	1.4	1.1	4	0	2	34	47	17	70
CL_{OETS}	Before				0	9	58	33	0	56
	After	1.2	1.1	4	0	3	36	46	15	68

a Calculated based on standard polystyrene

b Calculated based on ^{1}H NMR spectra

c Calculated based on the Q^n signal area of ^{29}Si NMR spectra

d $DC(\%)=0/4Q^0+1/4Q^1+2/4Q^2+3/4Q^3+4/4Q^4$

FTIR spectra of CLs are shown in Fig. 2. The adsorption bands due to υSi–H (2139 cm^{-1}), δCH_3 (approximately 1255 cm^{-1}), δSi–Me (approximately 1155 cm^{-1}), υCC (970 cm^{-1}), and ρSi–Me (903 cm^{-1}) were observed, indicating the completion of the silylation process [12, 16]. The absorption bands due to $\upsilon_{as}CH_3$ (approximately 2977 cm^{-1}), υ_sCH_2 (approximately 2930 cm^{-1}), υ_sCH_3 (approximately 2897 cm^{-1}), υCO (approximately 1100 cm^{-1}), υ_{as}Si–O–Si (approximately 1080 cm^{-1}), ρCH_3 in Si–CH_3 (860 cm^{-1}), υ_sSi–O–Si (795 cm^{-1}), and δCCO and δSiOSi (approximately 455 cm^{-1}) were also observed [11, 12, 17, 18].

Figure S1 presents the mass spectra of the CLs. These spectra indicate the presence of a variety of chemical species, spanning from trisiloxane to octasiloxane. However, precise interpretations of the CLs' mass spectra are challenging due to the existence of structures with overlapping molecular weights.

Figure 3 provides schematics of the anticipated structures of the CLs. Specifically, CL_{TEOS} primarily consists of cyclic siloxane derivatives, which, as a result of silylation, transition predominantly from Q^1 and Q^2 forms to Q^4. CL_{HEDS} is largely made up of 4-membered cyclic siloxane derivatives, transitioning chiefly from Q^2 to Q^4 due to silylation. Meanwhile, CL_{OETS} primarily consists of cyclic siloxane derivatives, converting mainly from Q^2 to both Q^3 and Q^4 as a result of the silylation process.

3.2 Properties of PDMS cross- linked with Si–H terminated TEOS, HEDS, and OETS oligomers (PDMS-CLs)

Figure 4a presents the FT-IR spectra of PDMS-CLs and PDMS-Vi acquired using the ATR method. Absorption bands corresponding to $\upsilon_{as}CH_3$ (2962 cm^{-1}), υ_sCH_2 (2903 cm^{-1}), δCH_3 in Si–CH_3 (1258 cm^{-}

^{1}), υ_{as}Si–O–Si (1075 cm^{-1}), υO–Si–O (1010 cm^{-1}), ρCH_3 in Si–CH_3 (860 cm^{-1}), both υSi–C and υ_{s}Si–O–Si (785 cm^{-1}), and υSi–C (700 cm^{-1}) were observed [11, 12, 17, 18]. Notably, no absorption band attributed to υSi–H (2139 cm^{-1}) was detected [12, 16]. The difference spectra between PDMS-CLs and PDMS-Vi, labeled as ΔPDMS–CL_{TEOS}, ΔPDMS–CL_{HEDS}, and ΔPDMS–CL_{OETS}, are depicted in Fig. 4b. The band corresponding to υC = C (1600 – 1500 cm^{-1}) exhibited a decrease, supporting the advancement of the hydrosilylation reaction [12, 19]. The absorption bands of the ethoxy group were discerned at ρCH_3 (1160 cm^{-1}), υC–O (1070 cm^{-1}), υC–C (970 cm^{-1}), and ρCH_2 (848 cm^{-1}) [12, 20, 21]. Strong bands associated with υ_{as}Si–O–Si (1060 cm^{-1}), υO–Si–O (1010 cm^{-1}), δSiCH_3 and υSiO_4 (780 cm^{-1}), and υSi–O (750 cm^{-1}) emerged, with the υO–Si–O (1010 cm^{-1}) and υSi–O (750 cm^{-1}) bands aligning with the PDMS chain [17, 18, 20].

Typically, the intensity and wavenumber of IR absorption are influenced by bonding angles, bond lengths, and adjacent conjugative interactions [14, 22, 23]. Moreover, changes in the Si–O distance and O–Si–O angle of the PDMS chain were observed following adsorption onto fumed silica [21]. Hence, PDMS–CLs likely demonstrate both inter- and intramolecular interactions between PDMS and the Q–unit moiety. A schematic detailing the preparation of PDMS–CLs is presented in Fig. 5.

The physical attributes of PDMS–CLs were assessed based on their transmittance, temperatures corresponding to 5% weight loss (T_{d5}), their swelling behavior in toluene, and tensile strength tests. Although PDMS–CLs displayed good transparency (≥ 80% at 500 nm), their appearance was tinted due to the inclusion of the Pt catalyst (as seen in Figure S2) [24].

Thermal properties were investigated using TGA in a nitrogen atmosphere. The TGA profiles of PDMS–Vi and PDMS–CLs are depicted in Fig. 6. It is established that the thermal degradation of PDMS under a nitrogen flow results in the formation of cyclic siloxanes like D_3 and D_4 through a depolymerization process [25]. Moreover, the residual ethoxy groups in PDMS–CLs undergo decomposition between 250–350°C [26–28]. Enhanced T_{d5} values were observed for PDMS–CLs in comparison to PDMS–Vi, an outcome attributed to the increased crosslink density [29, 30]. A similar trend was noticed under aerobic conditions, with T_{d5} results detailed in Table S1. The residual masses for PDMS–CLs followed the sequence 20wt% > 40wt% > 10%, with the exception of PDMS–CL_{TEOS}, which observed a sequence of 40wt% > 20wt% > 10%. When examining the 20wt% versions of the CLs, a minor peak around 600–700°C was identified, absent in the 20wt% PDMS–CLTEOS variant. Given that PDMS primarily depolymerizes from its chain ends, with heightened random main chain degradation at elevated temperatures in an inert environment [29], this peak is likely a reflection of that random degradation. Typically, increased crosslinking can inhibit random polymer main chain degradation [29, 31, 32]. Thus, it is inferred that CL_{HEDS} and CL_{OETS} possess superior crosslinking efficacy compared to CL_{TEOS}. However, variations in thermal degradation appeared minimal, potentially due to the structural similarities of the CLs. It is postulated that the thermal attributes of PDMS materials might be more influenced by the PDMS chain length than by the degree of crosslinking [7, 33–36].

To explore the mechanical reinforcement effects when incorporated with CLs, the tensile properties of PDMS–CLs were evaluated. The outcomes of the tensile strength tests are presented in Figure S3. The secant modulus value was determined from the tensile strength and strain values at the breaking point. The PDMS–CLs displayed low secant modulus and tensile strengths, ranging from 0.67 MPa (with 10wt% of CL_{TEOS}) to 1.4 MPa (with 40wt% of CL_{OETS}) and from 0.06 MPa (with 10wt% of CL_{TEOS}) to 0.96 MPa (with 40wt% of CL_{OETS}), respectively. The behavior of the secant modulus for PDMS–CLs is depicted in Fig. 7. As the content of CLs increased, the secant modulus values for PDMS–CLs also increased. Mackenzie et al. highlighted that the mechanical properties of PDMS–SiO_2 are influenced by the composition ratio between PDMS and silicates [37]. Furthermore, the secant modulus and tensile strength of PDMS materials are contingent upon the crosslinked network [33, 38]. Consequently, it is inferred that CP_{HEDS} and CP_{OETS} exhibit superior crosslinking efficiency compared to CL_{TEOS}, consistent with earlier findings.

Swelling tests for PDMS-CLs were conducted by measuring solvent uptake while stored in toluene at approximately 23°C for 3 days. The outcomes of these tests are presented in Fig. 8. No soluble fraction was detected in the swelling test, which validates that all PDMS CLs underwent reaction and cross-linking. The degree of swelling is inversely proportional to the extent of cross-linking; as the cross-linking degree increases, the swelling degree diminishes [11, 39–41]. As the content of CL increased, there was a corresponding decrease in the swelling degree. This trend suggests an escalation in the degree of cross-linking with increasing CL content. The solvent uptake for CLs decreased in the sequence: $CL_{TEOS} < CL_{HEDS} \leq CL_{OETS}$. Both CL_{HEDS} and CL_{OETS} are posited to exhibit superior cross-linking efficiency compared to CL_{TEOS}. This hypothesis stems from the presumed relation to the content of 4-membered cyclic siloxane derivatives and silylation on Q^3 silicon [10, 42].

All results are summarized in Table 2.

Table 2. Summary of physical properties of the elastomers prepared from PDMS–Vi and PDMS–CLs

CL	Content of CL (wt%)	Thickness (μm)	Transmittance[a] (%)	T_{d5}[b] (°C)	Residual mass[b] (%)	Swelling to toluene[c] (%)	Secant modulus (MPa)	Tensile strength (MPa)
none	0	-	-	364	5.5	-	-	-
CL_{TEOS}	10	199	80	478	19.8	720	0.067±0.003	0.06±0.0008
	20	110	87	427	44.8	595	0.24±0.13	0.18±0.04
	40	271	84	425	52.3	239	0.33±0.03	0.24±0.02
CL_{HEDS}	10	162	81	478	17.1	534	0.16±0.04	0.07±0.003
	20	156	87	460	63.7	394	0.24±0.03	0.12±0.04
	40	204	89	439	54.4	236	0.65±0.21	0.32±0.27
CL_{OETS}	10	148	86	447	24.3	519	0.16±0.05	0.086±0.06
	20	181	89	460	60.1	393	0.65±0.21	0.17±0.02
	40	183	85	446	55.2	213	1.4±0.52	0.96±0.45

[a]Measurement by UV-Vis spectra; the values are calculated at 500 nm

[b]Measurement by TG-DTA: T_{d5}: temperatures of 5% weight loss

[c]Solvent uptake calculated as 100 × solvent (g)/film (g)

4 Conclusion

The Si-H terminated ethoxyoligosiloxanes (CLs) were employed as cross-linkers for DQ silicone elastomers. All CLs exhibited a similar M_w (around 1400 Da), M_w/M_n (1.1), and OEt/Si-H ratio (4). However, their structures varied: CL_{TEOS} was primarily composed of cyclic siloxane derivatives silylated on Q^4 silicon; CL_{HEDS} mainly consisted of 4-membered cyclic siloxane derivatives silylated on Q^4 silicon; and CL_{OETS} predominantly comprised cyclic siloxane derivatives silylated on both Q^3 and Q^4 silicon. The effects of these distinct cross-linker structures were assessed in terms of transmittance, thermal stability, tensile strength, and swelling in toluene. Based on these evaluations, CL_{HEDS} and CL_{OETS} appear to offer superior cross-linking efficiency compared to CL_{TEOS}. These differences are believed to arise from the content of 4-membered cyclic siloxane derivatives and the silylation on Q^3 silicon. Thus, it is inferred that the properties of the elastomers are significantly influenced by the structures of the cross-linkers.

Declarations

ORCID ID

Yohei Sato: 0000-0003-2593-2720

Ryohei Hayami: 0000-0002-7005-7972

Kazuki Yamamoto: 0000-0001-6861-3944

Takahiro Gunji: 0000-0002-4658-6882

CrediT authorship contribution statement

Yohei Sato: Investigation, conceptualization, visualization, methodology, writing–original draft. **Ryohei Hayami**: Writing–review and editing, visualization. **Kazuki Yamamoto**: Supervision. **Takahiro Gunji**: Writing–review and editing, conceptualization, and supervision.

Compliance with ethical standards

Conflict of interest: The authors declare that they have no conflicts of interest.

Acknowledgements

This study was supported by the Japan Science and Technology Agency (JST) for the establishment of university fellowships toward the creation of science technology innovation (grant number: JPMJFS2144) and JSPS KAKENHI grants (grant number: 23KJ1965).

References

1. Kuo SW (2022) Hydrogen bonding interactions in polymer/polyhedral oligomeric silsesquioxane nanomaterials. J Polym Res 29:69. https://doi.org/10.1007/s10965-021-02885-4
2. Chujo Y (1996) Organic—inorganic hybrid materials. Curr. Opin. Solid State Mater. Sci., 6: 806–811. https://doi.org/10.1016/S1359-0286(96)80105-7
3. Mammeri F, Bourhis E L, Rozes L, Sanchez C (2005) Mechanical properties of hybrid organic–inorganic materials. J. Mater. Chem. 15: 3787–3811 https://doi.org/10.1039/B507309J
4. Sanchez C, Julia´n B, Belleville P, Popall M (2005) Applications of hybrid organic–inorganic nanocomposites. J. Mater. Chem. 15: 3559–3592 https://doi.org/10.1039/B509097K
5. Gunji T, Sakai Y, Suyama Y, Arimitsu K, Abe Y, West R (2004) Preparation and Properties of C60-Polysiloxane Hybrids. J Sol–Gel Sci. Technol. 32:43–46. https://doi.org/10.1007/s10971-004-5762-z
6. Gunji T, Shioda T, Tsuchihara K, Seki H, Kajiwara T, Abe Y (2010) Preparation and properties of poly oligomeric silsesquioxane/polysiloxane copolymers. Appl Organom Chem Soc 24:545–550 https://doi.org/10.1002/aoc.1562
7. Hayami R, Wada K, Nishikawa I, Sagawa T, Yamamoto K, Tsukada S, Gunji T (2017) Preparation and properties of organic–inorganic hybrid materials using titanium phosphonate cluster. Polymer J 49: 665–669 https://doi.org/10.1038/pj.2017.34
8. Gunji T, Itagaki S, Kajiwara T, Abe Y, Hatakeyama T, Aoki R (2009) Preparation and Properties of Siloxane/Epoxy Organic-Inorganic Hybrid Thin Films, Self-Standing Films, and Bulk Bodies. Polym J 41: 541–546 https://doi.org/10.1295/polymj.PJ2008290
9. Sato Y, Sugimoto A, Iwashina T, Hayami R, Yamamoto K, Gunji T (2023) Hydrolysis and condensation behavior of tetraethoxysilane, hexaethoxydisiloxane, and octaethoxytrisiloxane. J. Sol–Gel Sci. Technol. accepted.

10. Meshkov I B, Kalinina A A, Gorodov V V, Bakirov A V, Krasheninnikov S V, Chvalun S N, Muzafarov A M (2021) New principles of polymer composite preparation. MQ copolymers as an active molecular filler for polydimethylsiloxane rubbers. Polymers 13:2848. https://doi.org/10.3390/polym13172848
11. Hayami R, Nishikawa I, Hisa T, Nakashima H, Sato Y, Ideno Y, Sagawa T, Tsukada S, Yamamoto K, Gunji T (2018) Preparation and characterization of stable DQ silicone polymer sols. J Sol–Gel Sci. Technol. 88:660–670. https://doi.org/10.1007/s10971-018-4839-z
12. Sato Y, Hayami R, Gunji T (2022) Characterization of NMR, IR, and Raman spectra for siloxanes and silsesquioxanes: a mini review. J. Sol–Gel Sci. Technol. 104:36–52. https://doi.org/10.1007/s10971-022-05920-y
13. Kelts LW, Armstrong NJ (1989) A silicon-29 NMR study of the structural intermediates in low pH sol-gel reactions. J. Mater. Res. 4:423–433. https://doi.org/10.1557/JMR.1989.0423
14. Hook RJ (1996) A 29Si NMR study of the sol-gel polymerisation rates of substituted ethoxysilanes. J. Non–Cryst. Solids 195:1–15. https://doi.org/10.1016/0022-3093(95)00508-0
15. Unger B, Jancke H, Hähnert M, Stade H (1994) The early stages of the sol-gel processing of TEOS. J Sol-Gel Sci. Technol. 2:51–56. https://doi.org/10.1007/BF00486212
16. Gunji T, Igarashi T, Tsukada S, Abe Y (2017) Syntheses of cage octasilicate polymers. J. Sol–Gel Sci. Technol. 81:21–26. https://doi.org/10.1007/s10971-016-3998-z
17. Barthel H, Nikitina E (2002) INS and IR study of intermolecular interactions at the fumed silica-polydimethylsiloxane interphase, Part I. Polydimethylsiloxane models. Silicon Chem 1:239–247. https://doi.org/10.1023/B:SILC.0000018351.78847.f7
18. Barthel H, Nikitina E (2002) INS and IR study of intermolecular interactions at the fumed silica-polydimethylsiloxane interphase, Part 3. Sicica-siloxane adsorption complexes. Silicon Chem 1:261–279. https://doi.org/10.1023/B:SILC.0000018353.32350.c9
19. Takamura N, Gunji T, Hatano H, Abe Y (1999) Preparation and properties of polysilsesquioxanes: polysilsesquioxanes and flexible thin films by acid-catalyzed controlled hydrolytic polycondensation of methyl- and vinyltrimethoxysilane. J Polym Sci, Part A: Polym Chem 37:1017–1026. https://doi.org/10.1002/(SICI)1099-0518(19990401)37:7%3C1017::AID-POLA16%3E3.0.CO;2-F
20. Rubio F, Rubio J, Oteo JL (1998) A FT-IR Study of the Hydrolysis of Tetraethoylorthosilicate (TEOS). Spectr. Lett. 31:199–219. https://doi.org/10.1080/00387019808006772
21. Richards RE, Thompson HW (1949) Infra-red spectra of compounds of high molecular weight. Part IV. Silicones and related compounds. J Chem Soc 1949:124–132. https://doi.org/10.1039/JR9490000124
22. Weinhold F, West R (2011) The nature of the silicon–oxygen bond. Organometallics 30:5815–5824. https://doi.org/10.1021/om200675d
23. Weinhold F, West R (2013) Hyperconjugative interactions in permethylated siloxanes and ethers: the nature of the SiO bond. J Am Chem Soc 135:5762–5767. https://doi.org/10.1021/ja312222k
24. Lewis L N, Colborn R E, Grade H, Bryant Jr G L, Sumpter C A, Scott R A (1995) Mechanism of formation of platinum (0) complexes containing silicon–vinyl ligands. Organometallics 14:2202–

2213. https://doi.org/10.1021/om00005a021

25. Camino G, Lomakin S M, Lazzari M (2001) Polydimethylsiloxane thermal degradation Part 1. Kinetic aspects. Polymer 42:2395–2402. https://doi.org/10.1016/S0032-3861(00)00652-2
26. Takamura N, Taguchi K, Gunji T, Abe Y (1999) Preparation of Silicon Oxycarbide Ceramic Films by Pyrolysis of Polymethyl- and Polyvinylsilsesquioxanes. J Sol–Gel Sci. Technol. 16:227–234. https://doi.org/10.1023/A:1008765103113
27. Abe Y, Kagayama K, Takamura N, Gunji T, Yoshihara T, Takahashi N (2000) Preparation and properties of polysilsesquioxanes. Function and characterization of coating agents and films. J Non–Cryst Solids 261:39–51. https://doi.org/10.1016/S0022-3093(99)00614-6
28. Gunji T, Hayashi Y, Komatsubara A, Arimitsu K, Abe Y (2012) Preparation and properties of flexible free-standing films via polyalkoxysiloxanes by acid-catalyzed controlled hydrolytic polycondensation of tetraethoxysilane and tetramethoxysilane. Appl. Organomet. Chem. 26:32–36. https://doi.org/10.1002/aoc.1861
29. Chen D, Yi S, Wu W, Zhong Y, Liao J, Huang C, Shi W (2010) Synthesis and characterization of novel room temperature vulcanized (RTV) silicone rubbers using vinyl-POSS derivatives as cross linking agents. Polymer, (2010) 51:3867–3878. https://doi.org/10.1016/j.polymer.2010.06.028
30. Camino G, Lomakin S M, Lazzari M (2001) Thermal polydimethylsiloxane degradation. Part 2. The degradation mechanisms. Polymer 43:2011–2015. https://doi.org/10.1016/S0032-3861(01)00785-6
31. Tanaka K, Adachi S, Chujo Y (2009) Structure–property relationship of octa-substituted POSS in thermal and mechanical reinforcements of conventional polymers. J Polym Sci A: Polym Chem 47:5690–5697. https://doi.org/10.1002/pola.23612
32. Sato Y, Hayami R, Miyase Y, Ideno Y, Yamamoto K, Gunji T (2020) Preparation and properties of methyl- and cyclohexylsilsesquioxane oligomers as organic–inorganic fillers. J Sol–Gel Sci. Technol. 95:474–481. https://doi.org/10.1007/s10971-020-05291-2
33. Yamamoto K, Shimoda T, Sato Y, Nakaya T, Ohshita J, Gunji T (2022) Preparation and film properties of polysiloxanes consisting of di- and quadra-functional hybrid units. J Sol–Gel Sci. Technol. 104:724–734. https://doi.org/10.1007/s10971-022-05806-z
34. Grassie N, MacFarlane J (1978) The thermal degradation of polysiloxanes—I. Poly (dimethylsiloxane) Eur Polym J 14:875–884. https://doi.org/10.1016/0014-3057(78)90084-8
35. Grassie N, MacFarlane J, Francey K F (1979) The thermal degradation of polysiloxanes—II. Poly (methylphenylsiloxane). Eur Polym J 15:415–422. https://doi.org/10.1016/0014-3057(79)90053-3
36. Han Y, Zhang J, Shi L, Qi S, Cheng J, Jin R (2008) Improvement of thermal resistance of polydimethylsiloxanes with polymethylmethoxysiloxane as crosslinker. Polym. Degrad. Stab. 93:242–251. https://doi.org/10.1016/j.polymdegradstab.2007.09.010
37. Mackenzie J.D., Huang Q, Iwamoto T (1996) Mechanical properties of ormosils. J Sol–Gel Sci. Technol. 7:151–161. https://doi.org/10.1007/BF00401034
38. Liu M, Sun J, Sun Y, Bock C, Chen Q (2009) Thickness-dependent mechanical properties of polydimethylsiloxane membranes. J. Micromech. Microeng. 19:035028.

http://dx.doi.org/10.1088/0960-1317/19/3/035028

39. Sawvel A M, Chinn S C, Gee M, Loeb C K, Maiti A, Mason H E, Maxwell R S, Lewicki J P (2019) Nonideality in silicone network formation via solvent swelling and ^{1}H double-quantum NMR. Macromolecules 52:410–419. https://doi.org/10.1021/acs.macromol.8b01939
40. Sawvel AM, Crowhurst JC, Mason HE, Oakdale JS, Ruelas S, Eshelman HV, Maxwell RS (2021) Spectroscopic signatures of MQ-resins in silicone elastomers. Macromolecules 54:4300–4312. https://doi.org/10.1021/acs.macromol.1c00086
41. Fan X, Cao X, Shang X, Zhang X, Huang C, Zhang J, Zheng K, Ma Y (2021) Polym. Chem. A transparent cyclo-linear polyphenylsiloxane elastomer integrating high refractive index, thermal stability and flexibility. 12:5149–5158. https://doi.org/10.1039/D1PY00688F

Schemes

Scheme 1 is available in the Supplementary Files section

Figures

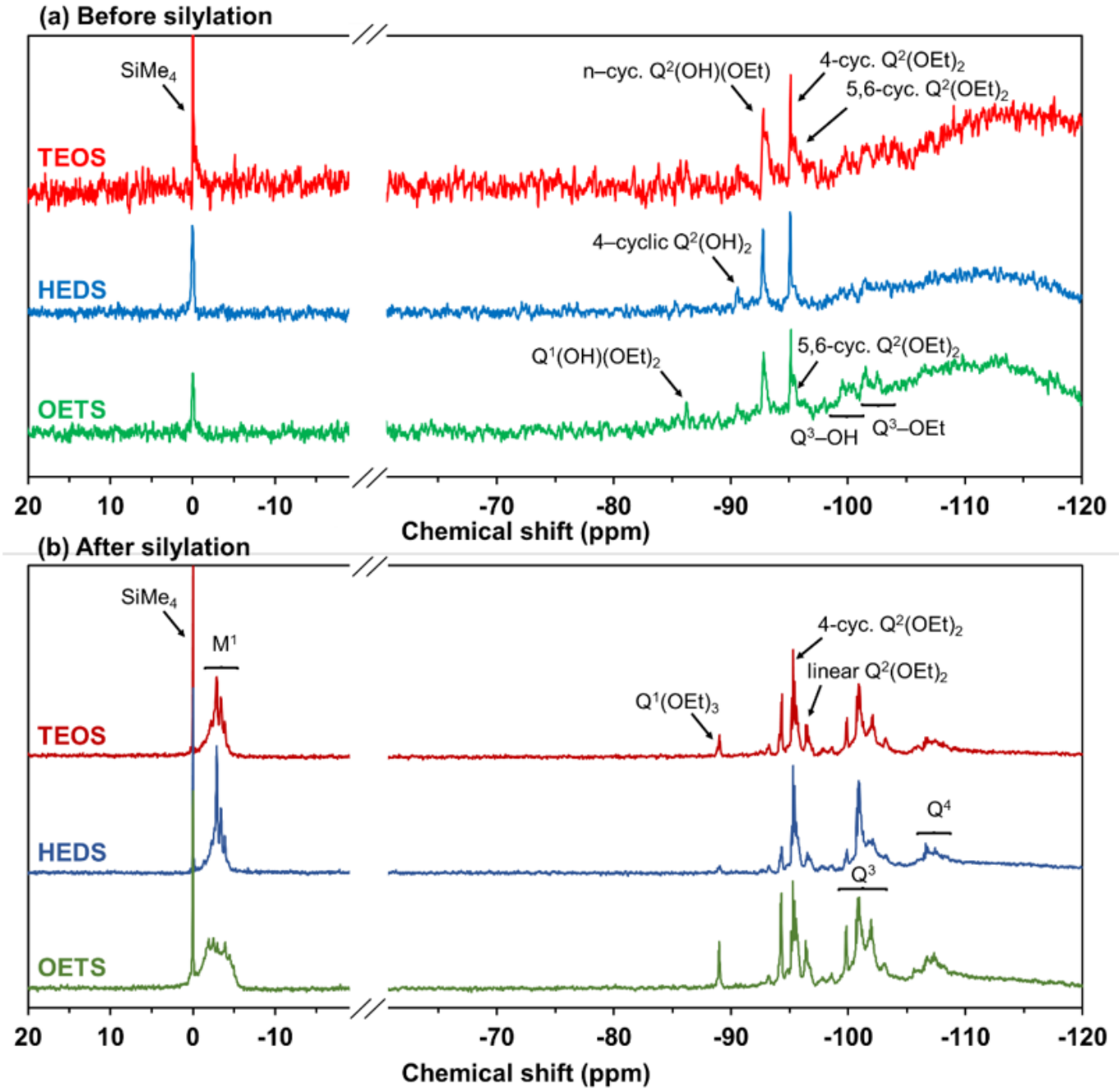

Figure 1

$^{29}Si\{^{1}H\}$ NMR spectra of TEOS, HEDS, and OETS hydrolysis condensate (a) before and (b) after silylation.

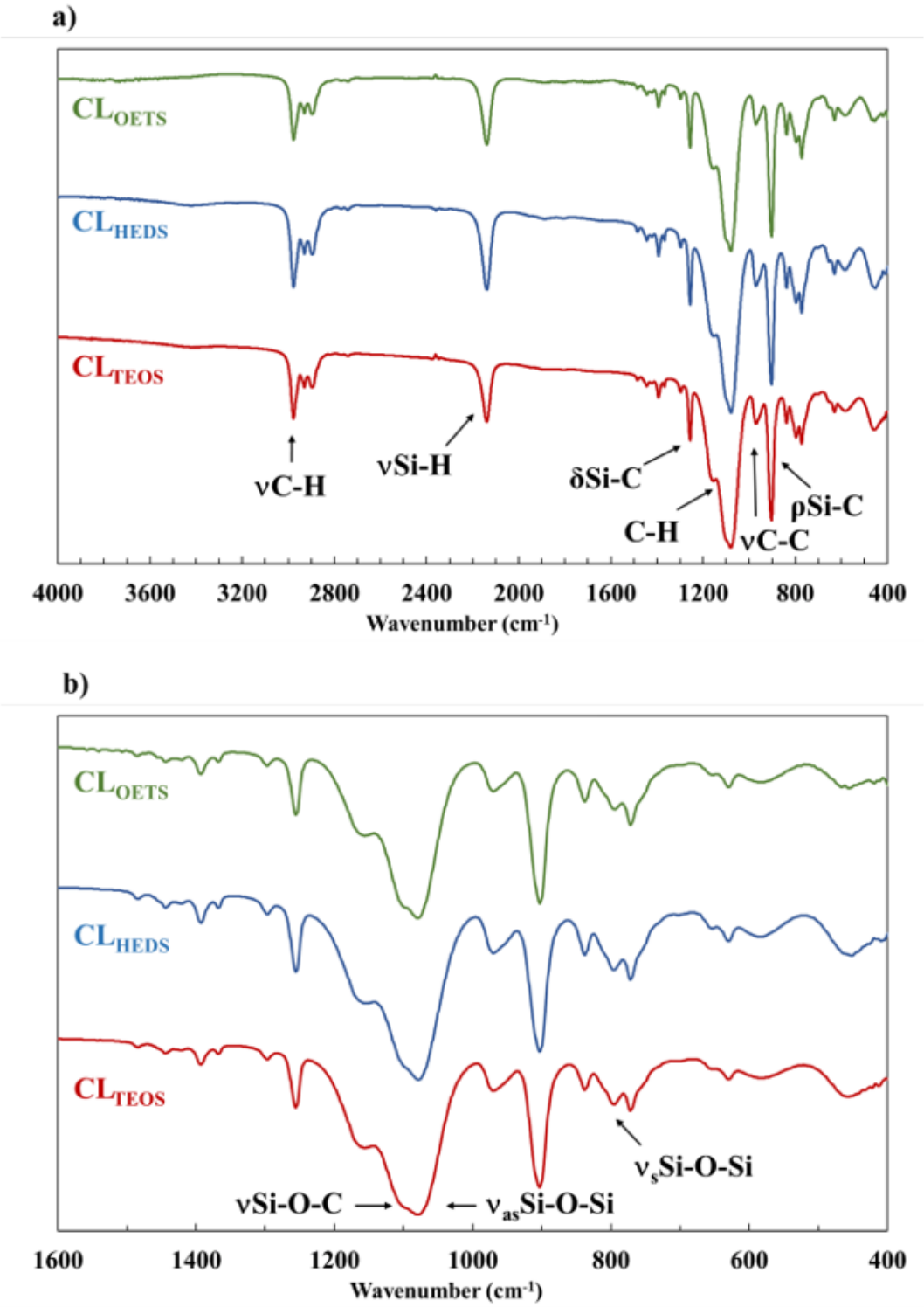

Figure 2

FTIR spectra of CLs. a) 4000–400 cm^{-1} region and b) 1600–400 cm^{-1} region.

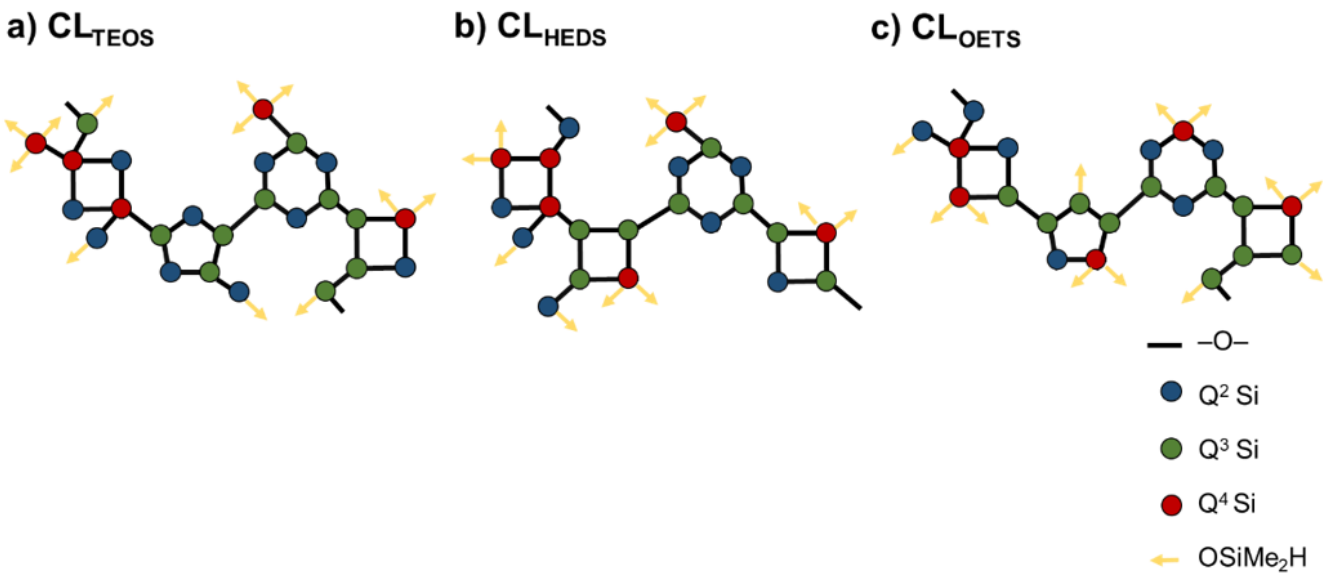

Figure 3

Schematics of estimated structures of a) CL_{TEOS}, b) CL_{HEDS}, and c) CL_{OETS}.

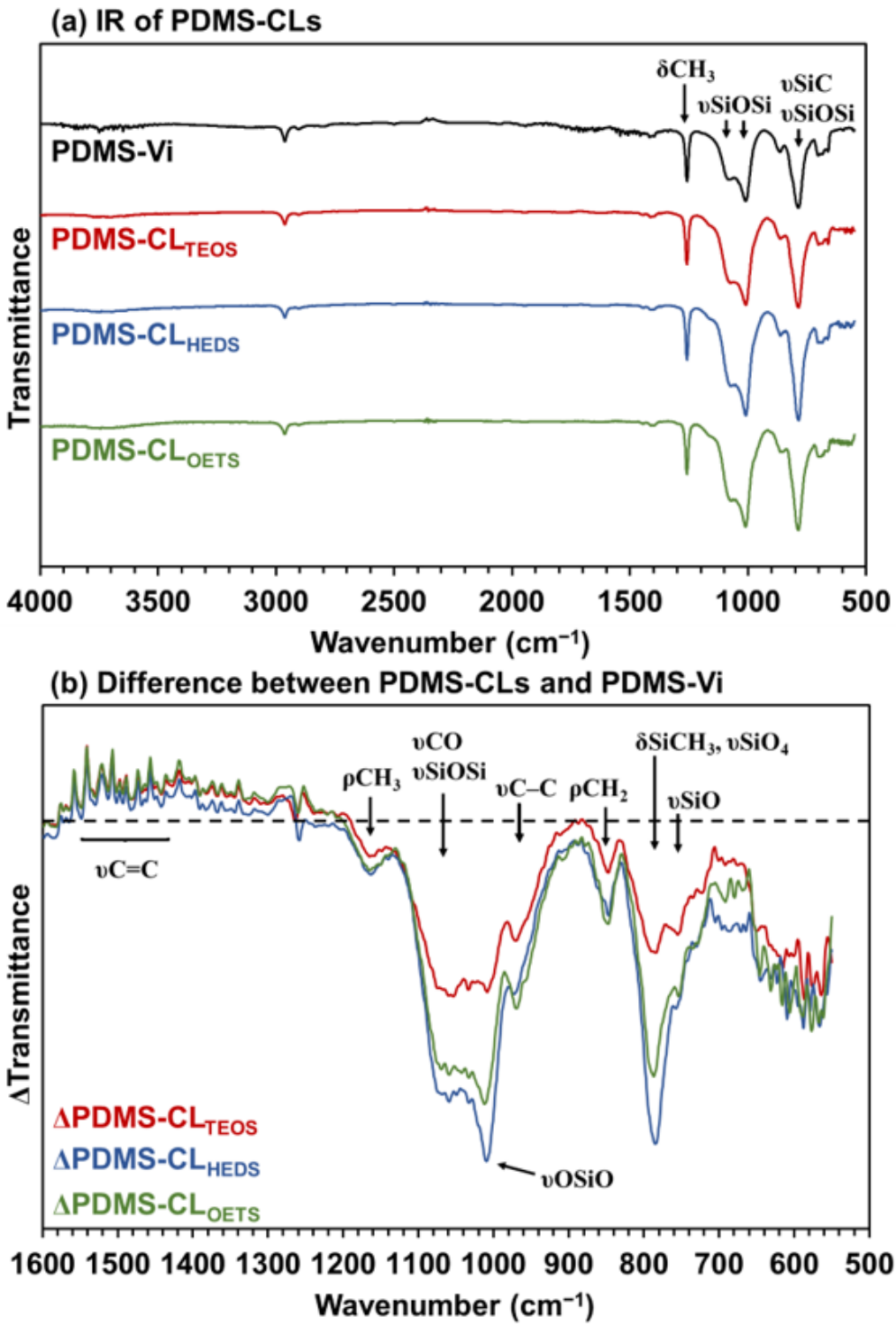

Figure 4

FTIR spectra of PDMS–Vi and 40-wt% PDMS–CLs via ATR method.

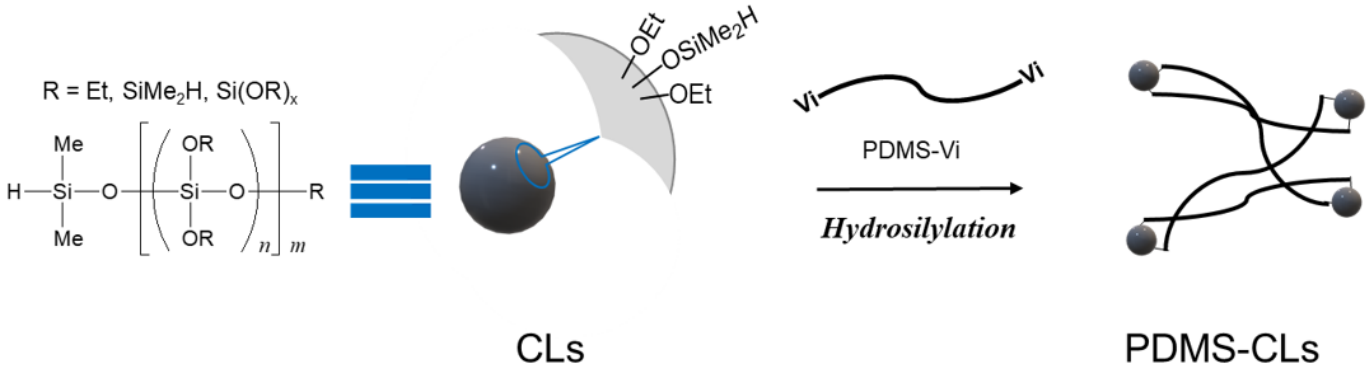

Figure 5

Schematic of preparation of PDMS–CLs.

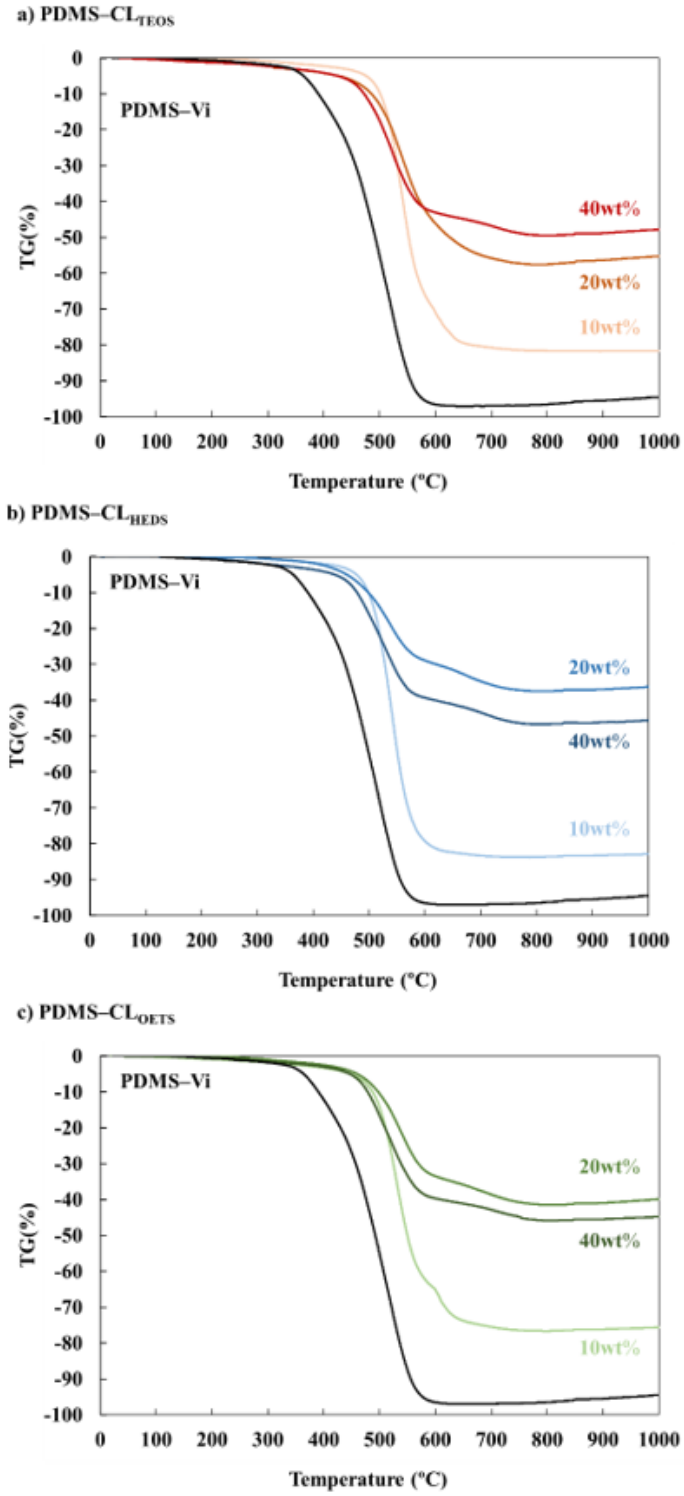

Figure 6

TGA traces of PDMS–Vi and a) PDMS–CL_{TEOS}, b) PDMS–CL_{HEDS}, and c) PDMS–CL_{OETS} under a nitrogen flow.

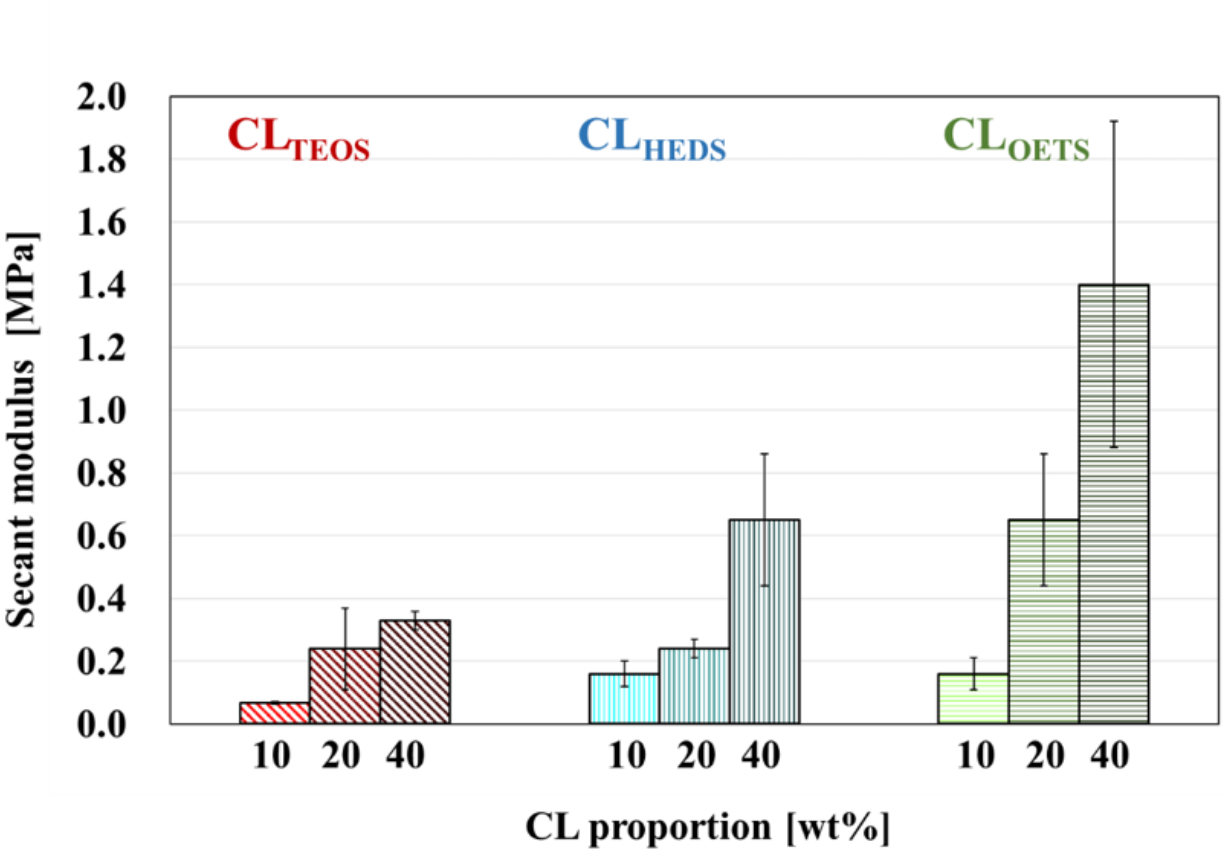

Figure 7

Secant modulus behavior of elastomers.

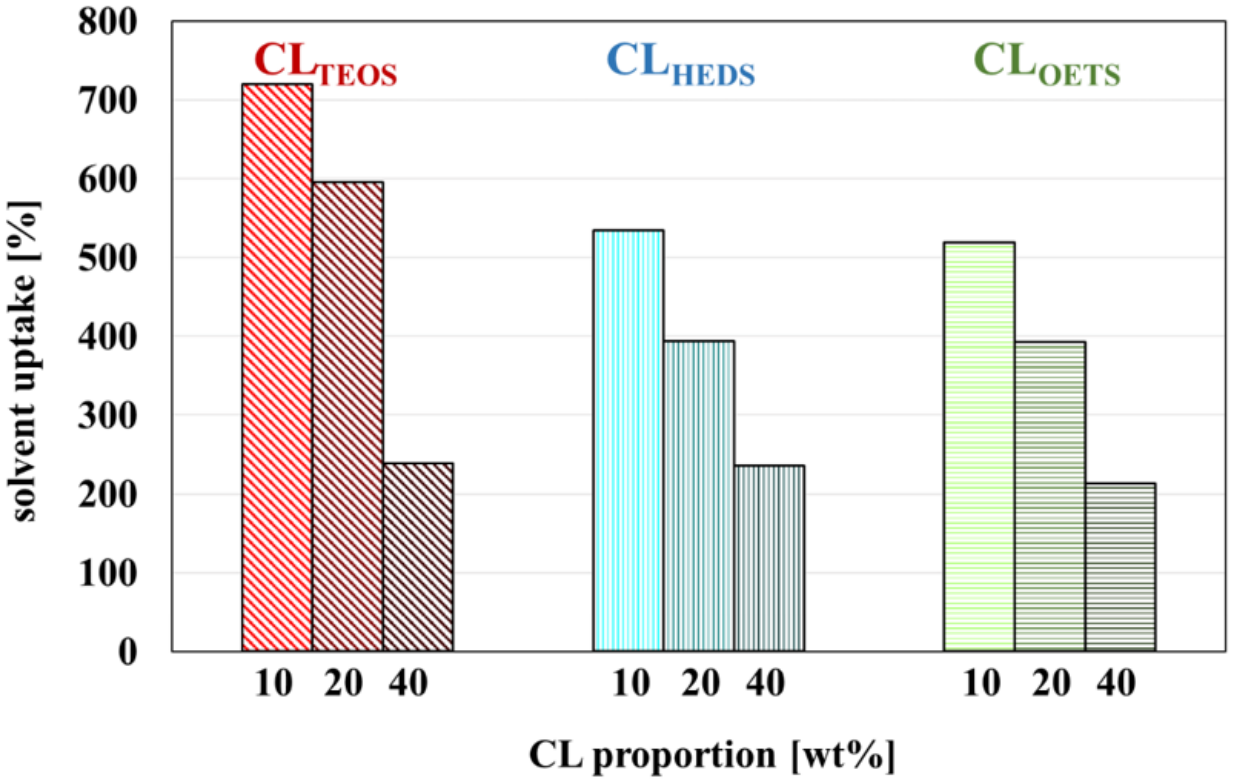

Figure 8

Swelling behavior of elastomers after storage in toluene for 3 days.

Supplementary Files

This is a list of supplementary files associated with this preprint. Click to download.

- GA.png
- SupportingInformation3RH.docx
- Scheme1.png